



HAL
open science

The Photoexcited Triplet State of Chlorophyll d in Methyl-tetrahydrofuran studied by Optically Detected Magnetic Resonance and Time-Resolved EPR

Marilena Di Valentin, Donatella Carbonera

► **To cite this version:**

Marilena Di Valentin, Donatella Carbonera. The Photoexcited Triplet State of Chlorophyll d in Methyl-tetrahydrofuran studied by Optically Detected Magnetic Resonance and Time-Resolved EPR. *Molecular Physics*, 2008, 105 (15-16), pp.2109-2117. 10.1080/00268970701627797. hal-00513140

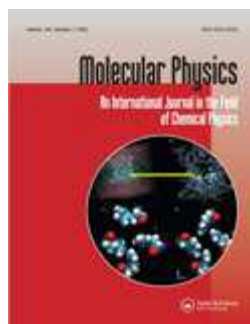
HAL Id: hal-00513140

<https://hal.science/hal-00513140>

Submitted on 1 Sep 2010

HAL is a multi-disciplinary open access archive for the deposit and dissemination of scientific research documents, whether they are published or not. The documents may come from teaching and research institutions in France or abroad, or from public or private research centers.

L'archive ouverte pluridisciplinaire **HAL**, est destinée au dépôt et à la diffusion de documents scientifiques de niveau recherche, publiés ou non, émanant des établissements d'enseignement et de recherche français ou étrangers, des laboratoires publics ou privés.



**The Photoexcited Triplet State of Chlorophyll d in Methyl-tetrahydrofuran
studied by Optically Detected Magnetic Resonance and Time-Resolved
EPR**

Journal:	<i>Molecular Physics</i>
Manuscript ID:	TMPH-2007-0207.R1
Manuscript Type:	Full Paper
Date Submitted by the Author:	26-Jul-2007
Complete List of Authors:	Di Valentin, Marilena; università di Padova carbonera, Donatella; università di Padova
Keywords:	chlorophyll, ODMR, FDMR, photosystem, TR-EPR



Only

1
2
3
4
5
6
7
8
9
10
11
12
13
14
15
16
17
18
19
20
21
22
23
24
25
26
27
28
29
30
31
32
33
34
35
36
37
38
39
40
41
42
43
44
45
46
47
48
49
50
51
52
53
54
55
56
57
58
59
60

The Photoexcited Triplet State of Chlorophyll *d* in Methyl-tetrahydrofuran studied by Optically Detected Magnetic Resonance and Time-Resolved EPR

Marilena Di Valentin^{a*}, Stefano Ceola^a, Giancarlo Agostini^b, Alison Telfer^d, James Barber^d, Felix Böhles^c, Stefano Santabarbara^c, Donatella Carbonera^{a*}

^a*Dipartimento di Scienze Chimiche, Università di Padova, Via Marzolo 1, 35131, Padova, Italy*

^b*Consiglio Nazionale della Ricerca, Istituto di Chimica Biomolecolare, Sezione di Padova, via Marzolo 1, 35131 Padova, Italy*

^c*School of Biological and Chemical Sciences, Queen Mary, University of London, Mile End Road, E1 4NS, London, United Kingdom*

^d*Division of Molecular Biosciences, Imperial College London, Biochemistry Building, South Kensington Campus, London SW7 2AZ, United Kingdom*

*to whom correspondence should be addressed:

e-mail: marilena.divalentin@unipd.it, donatella.carbonera@unipd.it

Abbreviations

Chl, chlorophyll; FDMR or ODMR, fluorescence or optically detected magnetic resonance; PS, photosystem; TR-EPR, time resolved electron paramagnetic resonance

Abstract

Chlorophyll *d* (Chl *d*) is the major pigment in the antenna proteins of both photosystems (PSI and II) of the oxyphotobacterium *Acaryochloris marina*. This fact suggests that photosynthesis based upon Chl *d* rather than Chl *a* may be an interesting alternative in oxygenic photosynthesis. While a great deal of spectroscopic information relative to Chl *a*, are available, both *in vivo* and *in vitro*, the literature on Chl *d* is scarce. In particular, the triplet state of Chl *d* has not been studied *in vitro* up to date. Although triplet states do not represent the main excitation path in the photosynthetic process they are involved in light stress events both in the antenna complexes and in the reaction centers and may also be used as endogenous paramagnetic probes of the molecular environment.

In this paper we make use of both time-resolved EPR and ODMR to characterize, for the first time, the Chl *d* triplet state in the polar solvent methyl-tetrahydrofuran. The comparison with the spectra of Chl *a* obtained under the same experimental conditions is also discussed.

Formatted

Formatted

Formatted

Formatted

Formatted

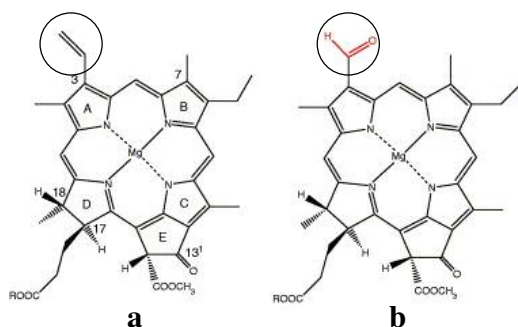
Formatted

1. Introduction

Chlorophyll (Chl *a*) is the dominant pigment in most oxygenic photosystems, acting both as a light harvesting pigment, in the inner and the peripheral antenna complexes, and as the primary electron donor in the reaction centres of Photosystem I (PSI) and Photosystem II (PSII). Chl *b* and *c* are found in the antenna complexes of higher plants and brown algae, respectively, but are not involved in photochemical pathways in the reaction centres. Hence, there has been a substantial consensus that Chl *a* is necessary to drive oxygenic photosynthesis. However, the ubiquitous role of Chl *a* has come under scrutiny when a the novel oxyphotobacterium *Acaryochloris marina* possessing Chl *d* in excess of 90% of the total chlorophyll was discovered [1]. Chl *d* in *A. marina* is not only the major pigment in the antenna proteins of both photosystems (PSI and II) [2] [3] but also acts as the primary donor in PSI, forming a special pair (either a Chl *d* dimer or a Chl *d*/Chl *d'* heterodimer) analogously to Chl *a* in PSI [2,4]. Despite the chemical difference in the primary donor in the PSI reaction centre of *A. marina* the kinetics of electron transfer and the chemical nature of secondary and successive electron transfer intermediates appear to be well conserved, compared to Chl *a* binding reaction centres of higher plants and cyanobacteria [5]. The role of Chl *d* in the reaction centre of *A. marina* is still a matter of debate. Evidence for Chl *d* acting as the primary donor has been recently reported by Okubo *et al.* [6]. On the other hand, Telfer and coworkers [7] suggested that is Chl *a* which acts as the primary donor in PSII reaction centre of *A. marina*. However a role as an electron transfer intermediate for Chl *d* was not ruled out in this latter study. Hence, photosynthetic oxygen evolution based mainly upon Chl *d* rather than Chl *a* constitutes an interesting alternative in oxygenic photosynthesis.

1
2
3
4
5
6
7
8
9
10
11
12
13
14
15
16
17
18
19
20
21
22
23
24
25
26
27
28
29
30
31
32
33
34
35
36
37
38
39
40
41
42
43
44
45
46
47
48
49
50
51
52
53
54
55
56
57
58
59
60

In the Chl *d* molecule the divinyl group which is present in ring A of Chl *a* is replaced by a formyl group (Scheme 1). The proposed structure for Chl *d*, produced by oxidation as 2-desvinyl-2-formyl-chlorophyll-*a*, was provided in 1959 by Holt *et al.* [8]. Chl *d* differs markedly from all the other chlorophylls in having the Q_y absorption peak in the near infrared. The optical spectral properties of Chl *d* are, therefore, unique. The Q_y electronic transition of Chl *d* in acetone is characterized by an absorption peak at 691 [8-9], which is about 30 nm red-shifted compared to Chl *a* in the same organic solvent [10]. An even more pronounced red-shift of the absorption is observed *in vivo* where absorption transitions in the 708–720 nm range were observed [1]. Therefore, it has been hypothesised that the presence of Chl *d* as the principal pigment in *A. marina* is the result of adaptation to the peculiar environmental niche in which the organism resides, [2, 11], forming biofilms on the underside of didemnid ascidians [12]. This adaptation hypothesis is supported by the similarity of the electron transfer reactions in PSI of *A. marina* compared to those of Chl *a* binding organisms and the high homology of the all the reaction centre subunits [13]. In order to understand the role of the Chl *d* in energy transfer and electron transfer processes in the photosynthetic apparatus of *A.* it is necessary, in the first place, to acquire detailed information on the electronic and spectroscopic properties of Chl *d*.



1
2
3
4
5
6
7
8
9
Scheme 1. Molecular structure of (a) chlorophyll *a* and (b) chlorophyll *d*. The divinyl group in ring A of chlorophyll *a* is replaced by a formyl group in chlorophyll *d* (highlighted).

10
11
12
13
14
15
16
17
18
19
20
21
22
23
24
25
26
27
28
29
30
31
32
33
34
35
36
37
38
39
40
41
42
43
While singlet excited states of chlorophylls are directly involved in energy and electron transfer processes leading to energy conversion, excited triplet states do not take part in the main path of photosynthesis. Thus the Chl triplet, which in chlorophyll in organic solvent has a yield of around 60% (see [14] for a review), is of little direct importance in photosynthetic energy conversion. However, it plays a primary role during the light-induced stress, a phenomenon which goes under the name of photoinhibition. In the photosynthetic complexes, the triplet states of Chl are populated by two mechanisms; intersystem crossing (ISC) from the lowest singlet excited states, analogous to pigment in solution, and from charge recombination of the primary radical pair. The rate of ISC, in isolated pigment protein complexes, is significant and of the same order of magnitude as that for the other decay processes [15]. Although within chlorophyll protein complexes Chl triplet levels are normally efficiently quenched by carotenoids (e.g. [16-18]), Chl triplets populated by ISC have been detected in many PSII enriched particles [19] and components, including outer [20,21] and inner antenna [22,23] complexes. More recently Chl triplet states populated by ISC were also detected in substantially intact systems such as isolated thylakoid membranes from spinach [24] and *Chlamydomonas reinhardtii* [5].

44
45
46
47
48
49
50
51
52
53
54
55
56
57
58
59
60
In the reaction centres Chl triplet states can be populated by charge recombination of the separated primary radical pair couple [25-28]. Charge recombination reactions are enhanced by the pre-reduction of the terminal acceptors of the reaction centres. Under this condition the lifetime of the primary radical pair is lengthened by order of magnitudes (ns vs. ps timescale), increasing the probability of charge recombination,

1
2 and population of the triplet state [26-28]. Therefore Chl triplet states are molecular
3 probes of processes which occur under high excitation pressure, i.e. light stress
4 conditions. Since, triplet states are paramagnetic (total spin $S=1$) they are suited for
5 investigation by electron paramagnetic resonance (EPR) spectroscopic techniques.
6
7

8
9
10 Until now EPR investigations concerning the photo-excited triplet state of Chl *d* have
11 not been reported. On the other hand, the triplet states of Chl *a* and Chl *b*, both *in vivo*
12 and *in vitro*, have been the subject of extensive investigations either by optical or by
13 EPR spectroscopy. Many studies of the Chl triplet states have been performed with the
14 aim of understanding the environmental effect induced by solvent polarity and axial
15 ligand coordination to the central magnesium on the spectroscopic properties of the
16 molecules [29-31]. In most of the initial studies the steady-state EPR spectra of the Chl
17 triplet states were recorded by amplitude modulation of the light excitation beam and
18 phase-sensitive detection of the spin polarized spectrum, using a lock-in amplifier. More
19 recently the triplet state of Chl has been investigated by Time-resolved EPR (TR-EPR).
20 In TR-EPR experiments the resonant microwave field is directly monitored and the time
21 evolution of the spin-polarized spectrum after the laser pulse excitation is recorded [32].
22 TR-EPR allows the spin-polarization pattern (ESP) of a triplet state to be directly
23 determined, because it is conducted in the absence of external field modulation. The
24 ESP cannot be unambiguously determined by CW-EPR, due to the admixture of the
25 signals arising from spin-polarized (non-Boltzmann) and equilibrated (Boltzmann)
26 states.
27
28
29
30
31
32
33
34
35
36
37
38
39
40
41
42

43
44 The zero-field splitting (ZFS) tensor and ESP are the most important parameters of
45 triplet-state EPR. The ZFS parameters (D and E) reflect the intensity of the magnetic
46 dipolar interaction between the unpaired electrons. D is related to the mean distance
47 between spins while E is related to the symmetry of the electronic distribution in the
48 molecular plane. ESP depends on the selective ISC rates to the three spin sublevels.
49
50
51
52
53
54
55
56
57
58
59
60

1
2
3
4
5
6
7
8
9
10
11
12
13
14
15
16
17
18
19
20
21
22
23
24
25
26
27
28
29
30
31
32
33
34
35
36
37
38
39
40
41
42
43
44
45
46
47
48
49
50
51
52
53
54
55
56
57
58
59
60

Because the triplet sublevels are already not degenerate in the absence of an externally applied magnetic field due to the dipole-dipole magnetic interaction between the unpaired spins, Optically Detected Magnetic resonance in Zero-Field (ZF-ODMR) constitutes an alternative and complementary analytical tool to EPR for the study of photo-excited triplet states of chromophores. Thus, ZF-ODMR, has also been used extensively to characterize Chl triplet states both *in vitro* and in photosynthetic systems [31,33]. ZF-ODMR is a double resonance technique based on the simple principle that, when under continuous illumination a triplet steady state population is generated, the application of a resonant microwave field between a couple of spin sublevels of the triplet state generally induces a change of the steady state population of the triplet state itself, due to the anisotropy of the decay and population rates of the three spin sublevels. The change induced in the triplet population may be detected as a corresponding change in the emission and/or absorption of the system [31]. In the FDMR experiments the fluorescence is collected in the presence and in the absence of the swept microwave field and the difference is amplified. In the absorption detection mode (ADMR) the excitation beam is focused into the monochromator after passing through the sample and is finally collected by a photodiode. By fixing the microwave frequency at a resonant value while sweeping the detection wavelength, Triplet-minus-Singlet (T-S) spectra can be registered. The advantage of the technique is the high sensitivity due to the detection of optical photons and the possibility to correlate, by site selection, the ZFS parameters to the optical properties of the species carrying the triplet state. Because the anisotropy of electron spin-spin dipolar interaction does not contribute to the magnetic resonance linewidth in the absence of a magnetic field and the hyperfine interactions do not broaden the ODMR lines at the first order, the ZFS parameters can be determined with high precision. In fact the peaks at the resonant frequency are very narrow compared to EPR.

1
2
3
4
5
6
7
8
9
10
11
12
13
14
15
16
17
18
19
20
21
22
23
24
25
26
27
28
29
30
31
32
33
34
35
36
37
38
39
40
41
42
43
44
45
46
47
48
49
50
51
52
53
54
55
56
57
58
59
60

In this paper we make use of both TREPR and ODMR to characterize, for the first time, the Chl *d* triplet state in the polar solvent methyl-tetrahydrofuran (Me-THF). The comparison with the spectra of Chl *a* obtained under the same experimental conditions is also discussed.

We consider this an important starting point for the characterization and analysis of Chl *d* triplet states *in vivo*.

Formatted

2. Materials and Methods

Extraction and purification of Chl d from A. marina cells. *A. marina* was grown on K+ESM medium as previously described [7]. Cells were harvested in the logarithmic growth phase by centrifugation at 1 500 *g* for 10 minutes. Pigments were extracted by resuspending the cell pellet in methanol, with a volume equivalent to ten times the cells weight, for 20 minutes, at 4 C in the dark. The suspension was then centrifuged for 10 minutes at 12000 *g* in a refrigerated centrifuge. The procedure was repeated until the cell pellet was seemingly colourless. The green supernatants were pooled together and transferred in a separating flask. Pigments were separated by adding a volume equal to the initial methanol extract of diethyl ether. The solution was washed three times with equal volumes of water. The diethyl ether layer was dried in a rotary evaporator and the powder resuspended in a minimal amount of 45:45:10 Acetonitrile: Methanol: Water mixture. Chl *d* was purified by HPLC using an Agilent 1100 series HPLC integrated unit equipped with a on-line diode array detector. The pigment extract was loaded on a C18 reverse phase column (Spherisorb 5 μ m ODS2-C18 (Phase Separation Ltd, Deeside), dimension 250 x 4.1 mm) and the pigment were separated by running consecutive linear gradients. The first gradient starting mixture of 45:45:10 Acetonitrile: Methanol: Water, was run by decreasing the water content linearly, at a flow rate of 1ml min⁻¹, to 50:50 Acetonitrile: Methanol final mixture. The second gradient was run

1
2 increasing the Acetonitrile concentration to 80% at the same flow rate. The pigment
3 elution profile was monitored at 420nm, 500nm, 673 nm and 683nm simultaneously.

4
5
6 Chl *d* eluted with the second gradient after 23.5 minutes, and Chl *a* after 25.1 minutes.

7
8 The concentration and the purity of Chl *d* were checked by absorption spectroscopy
9 with a Lambda 35 Perkin Elmer spectrometer. Chl *a* was purchased from SIGMA; the
10 Chl was dried carefully before dissolving it in the Me-THF solvent to remove all
11 residual water. The solvent was distilled from sodium before usage.

12
13
14
15
16 *ODMR measurements.* The samples were diluted in Me-THF to a final Chl
17 concentration of 10^{-5} M sealed in a capillary tube after several pumping/freezing cycles
18 in order to remove the oxygen from the sample. Cooling of the samples was done
19 slowly down to cryogenic temperature in the cryostat. Fluorescence detected magnetic
20 resonance (FDMR) and absorption detected magnetic resonance (ADMR) experiments
21 were performed in the same, home built, apparatus, previously described in detail
22 [22,34]. The flexibility of the set up allows performance of both kinds of experiments
23 on the same sample by switching the detection mode. Amplitude modulation of the
24 applied microwave field, used to greatly increase the signal to noise ratio, was done by
25 means of a phase sensitive lock-in amplifier (EG&G 5220). In the FDMR experiments
26 the fluorescence, excited by a halogen lamp (250 W) focused into the sample and
27 filtered by a broadband 5 cm solution of CuSO_4 1M, was collected at 45 degree through
28 appropriate cut-on or band-pass filters (10 nm FWHM) by a photodiode before entering
29 the lock-in amplifier. Low temperature emission spectra were detected in the same
30 apparatus used for ODMR experiments, using the same excitation source, but
31 substituting the band-pass filters before the photodiode, coupled to a voltage-amplifier,
32 by a monochromator. In the ADMR setup the same excitation lamp was used but
33 without filters before the sample, except for 5 cm water and other heat filters. The beam
34 was focused into the monochromator after passing the sample and finally collected by a
35
36
37
38
39
40
41
42
43
44
45
46
47
48
49
50
51
52
53
54
55
56
57
58
59
60

1
2 photodiode. The temperature was 1.8 K for most of the experiments. At such a
3
4 temperature spin-lattice relaxation is inhibited and the ODMR signal is maximum.
5

6
7 *TR-EPR measurements.* TR-EPR spectra were obtained in quadrature detection mode
8
9 with DC-AFC coupling using pulsed light excitation. The X-band EPR spectrometer
10 (Bruker Elexsys E580) was equipped with a EN4118X-MD4 X-band dielectric module
11 working at 9.7 GHz and a nitrogen flow system. The EPR experiments were performed
12
13 at 90 K. . The microwave power used for the TR-EPR experiments was about 2mW at
14
15 the cavity. Laser excitation at 532nm (10 mJ per pulse and repetition rate of 10 Hz) was
16
17 provided by the second harmonic of a Nd:YAG laser (Quantel Brilliant).
18
19

20
21 The time resolution of the TR-EPR spectrometer was 100 ns. No field modulation or
22
23 phase-sensitive detection was used. The EPR signals were taken from the quadrature
24
25 detection arm of the Super XFT bridge and sampled with the SpecJet, triggered by the
26
27 Q-switch. Transients were accumulated under off-resonance field conditions and
28
29 subtracted from those on resonance in order to eliminate the laser background signal.
30

Formatted

31
32 Simulations of the spin polarised triplet spectra were performed using a program written
33
34 in Matlab® with the aid of the Easyspin routine (ver. 2.6.0) [35].The program is based
35
36 on the full diagonalization of the spin Hamiltonian, taking into account the Zeeman and
37
38 magnetic dipole-dipole interactions, assuming a powder distribution of molecular
39
40 orientations with respect to the magnet field direction.
41
42

43 44 **3. Results**

45
46 The fluorescence emission spectra of Chl *d* and Chl *a* dissolved in Me-THF, detected at
47
48 1.8 K, are presented in figure 1. The fluorescence emission spectra of Chl *a* peaks at
49
50 673 nm and shows an intense low-energy vibrational band at 727 nm. The main
51
52 fluorescence emission band and the low-energy vibrational transition are red-shifted to
53
54
55
56
57
58
59
60

698 nm and 760 nm respectively, in the fluorescence emission spectrum of Chl *d*. The red shift of the Chl *d* fluorescence emission compared to that of Chl *a* is in agreement with previous observations of the emission spectra of these pigments recorded at 10 K in reconstituted complex of PCP [36]. It is also in agreement with the absorption spectrum of the pigments at 10 K in Me-THF which shows the main electronic transition at 670 nm for Chl *a* and at 697 nm for Chl *d* [36].

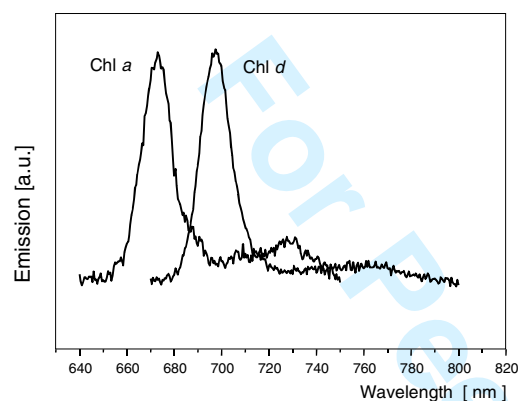


Figure 1. Normalized fluorescence emission spectra of Chl *a* and Chl *d* in Me-THF at 1.8 K. Broad band excitation (400-600 nm), resolution 1 nm.

The FDMR spectra taken at the maximum of the fluorescence are shown in figure 2. Only two of the three possible transitions were detected. They correspond to the $|D|-|E|$ and $|D|+|E|$ transitions. The $2|E|$ transition was too weak to be detected, as usually reported for Chl *a* and *b* triplet states. The $|D|-|E|$ transition of Chl *a* in Me-THF has a maximum at 740 MHz, while the $|D|+|E|$ transition shows a peak at 992 MHz. Instead, the $|D|-|E|$ transition of Chl *d* has a peak at 616 MHz, downshifted by 124 MHz compared to Chl *a*. As the linewidth (FWHM) of the $|D|-|E|$ resonance lines of Chl *a* and Chl *d* are 37.5 MHz and 40 MHz respectively, the two transitions do not overlap, and would be distinguishable in a Chl *a*/Chl *d* mixture, as it occurs *in vivo*. The $|D|+|E|$ transition of Chl *d* is observed at 906 MHz, and it is less separated from that of Chl *a*.

The corresponding ZFS parameters for both species are reported in table 1. The order of relative intensity of the transitions is the same for the two pigments, that is $|D|-|E| > |D|+|E| >> 2|E|$, although the difference among them is more pronounced for the Chl *d* triplet state.

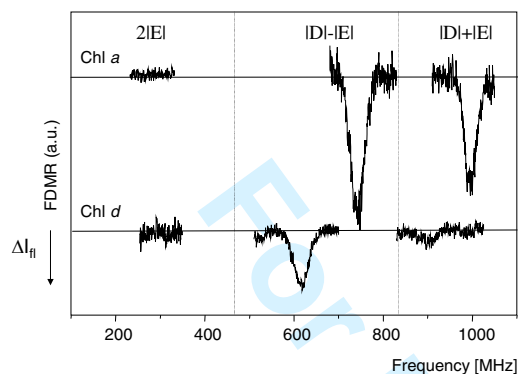


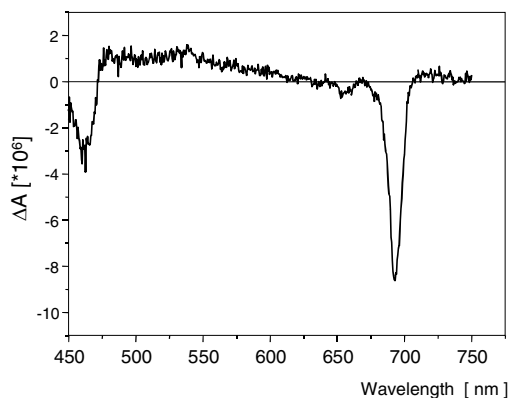
Figure 2. FDMR spectra of Chl *a* and Chl *d* in Me-THF at 1.8 K collected through a 10 nm band pass filter at emission wavelength near the maximum of the emission spectral forms shown in Figure 1: 670 nm for Chl *a* and 700 nm for Chl *d*. Spectral regions corresponding to $2|E|$, $|D|-|E|$, $|D|+|E|$ transitions are indicated. Microwave frequency modulation: 33 Hz; Microwave power, 0.6 mW. Number of scans: 30. The traces have been vertically shifted for an easier comparison.

ODMR					
	$ D - E $ (MHz)	$ D + E $ (MHz)	FWHM (MHz)	$ D $ (cm^{-1})	$ E $ (cm^{-1})
Chl <i>a</i>	740.0 ± 0.5	992.0 ± 0.5	40.0 ± 0.5	0.0289	0.0042
Chl <i>d</i>	616.0 ± 0.5	906.0 ± 0.5	40.5 ± 0.5	0.0254	0.0048
EPR					
	A_x	A_y	A_z	$ D $ (cm^{-1})	$ E $ (cm^{-1})
Chl <i>a</i>	0.33	0.56	0.11	0.0289	0.0042
Chl <i>d</i>	0.34	0.50	0.16	0.0259	0.0050

Table 1. ODMR: values of experimental resonant frequencies and of the calculated ZFS parameters (errors $\pm 0.0001 \text{ cm}^{-1}$).

TR-EPR: Relative population probabilities (A_x , A_y , A_z) and ZFS parameters (errors $\pm 0.0002 \text{ cm}^{-1}$) determined from spectral simulations.

By setting the resonance frequency at 616 MHz, the maximum value of the $|D| - |E|$ transition, the microwave-induced T-S spectrum of Chl *d* was recorded (see figure 3). The main absorption bleaching is centred at 693 nm and corresponds to the Q_y transition in the singlet manifold, while a bleaching in the Soret region is seen below 470 nm (close to the wavelength limit of the monochromator). The positive triplet-triplet absorption is a broad band covering the range between 450 and 700 nm. The general features of the T-S spectrum are very similar to those reported for Chl *a* in monomeric form [33], indicating that the main electronic structure of the Chl *d* triplet manifold is conserved with respect to Chl *a*. The absence of a positive contribution to the T-S spectrum in the region of the Q_y absorption is an indication that the species associated to the magnetic transition is not a Chl *d* dimer.



1
2
3
4
5
6
7
8
9
10
11
12
13
14
15
16
17
18
19
20
21
22
23
24
25
26
27
28
29
30
31
32
33
34
35
36
37
38
39
40
41
42
43
44
45
46
47
48
49
50
51
52
53
54
55
56
57
58
59
60

Figure 3. T-S spectrum of Chl *d* in Me-THF at 1.8 K detected at 616 MHz, the maximum of the $|D|-|E|$ transition detected by FDMR. Mod. freq. 323 Hz, Mw power 1W.

The ADMR spectrum obtained by selecting a detection wavelength at 693 nm, (the maximum bleach in the T-S spectrum) is presented in figure 4. It shows the same microwave transitions detected by FDMR, with the same relative intensity, confirming that the same triplet population is observed either by absorption or fluorescence emission.

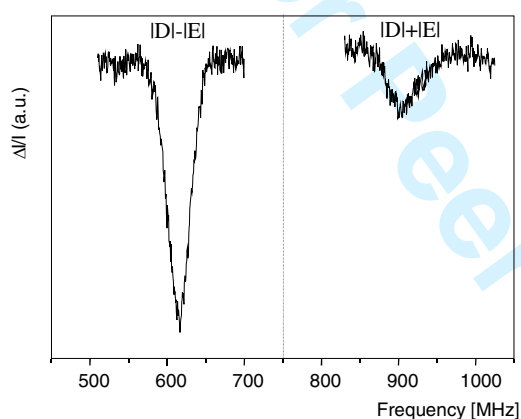


Figure 4. ADMR spectrum of Chl *d* in Me-THF at 1.8 K, recorded at 692.5 nm. Mod. freq. 33 Hz, Mw power 1W. Only the $|D|-|E|$, $|D|+|E|$ transitions are shown.

When performing FDMR on the Chl *d* triplet state by collecting the whole emission band (using a 650 nm cut-on filter) an additional peak at about 940 MHz, with opposite sign compared to that detected by the band pass filter at 700 nm, shows up (see figure 5). A corresponding $|D|-|E|$ transition is however not easily discerned in the spectrum. This additional transition may be due to the presence of a second minor population of triplet state. Unfortunately we were unable to measure either a specific emission

wavelength or an associated T-S spectrum of this second component because of the weakness of the corresponding signal.

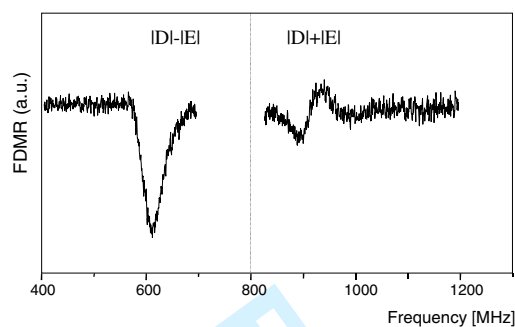


Figure 5. FDMR spectra of Chl *d* in Me-THF at 1.8 K, collected through a 630 nm cut-off filter. Spectral regions corresponding to $|D|-|E|$ and $|D|+|E|$ transitions are indicated. Microwave frequency modulation: 33 Hz; Microwave power, 0.6 mW. Number of scans: 25.

The laser-flash induced TR-EPR spectrum of Chl *d* in Me-THF at 90 K is shown in figure 6. The spectrum, recorded at 100ns after the laser flash, with an integration window of 60 ns, can be considered the initial spectrum, from the point of view of the ESP, because decay rate of the EPR transient signals is in microsecond range at low microwave power (data not shown). The polarization pattern of this initial powder spectrum is *eaeeae*. The ZFS parameters $|D|$ and $|E|$, obtained from spectral simulation, are in good agreement with the values derived from the ODMR experiments for the main triplet population. A comparison with the spectrum of Chl *a*, obtained in the same experimental conditions, is also shown in the same figure. The population probabilities at the three canonical field positions (X,Y,Z) and the ZFS parameters, obtained from the spectral simulations of the initial triplet spectra (shown in figure 6), are reported in table 1 for both molecules.

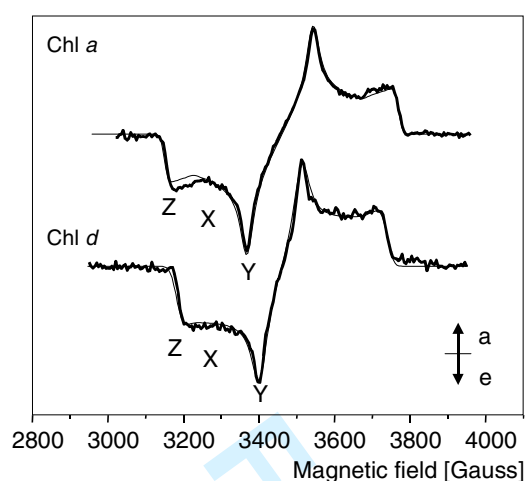


Figure 6. X-band triplet TREPR spectra of Chl *a* (top) and Chl *d* (bottom) in Me-THF at 100 ns after the laser pulse (thick line) and the corresponding spectral simulations (thin line). The simulation parameters are reported in table1. a = absorption, e = emission.

4. Discussion

As already stated in the Introduction, the discovery of the photosynthetic oxygenic organism *Acaryochloris marina*, containing Chl *d* rather than Chl *a* as its major pigment, has challenged the view that Chl *a* is necessary in order to perform oxygen evolution. Moreover, very recently the PCP antenna complex from the red alga *Dinoflagellate*, which contains two Chl *a* molecules surrounded by 8 peridinin, has been reconstituted *in vitro* with Chl *d*, to study the effect of the porphyrin electronic structure on the efficiency of the energy transfer [36-38]. We have studied this reconstituted complex in terms of triplet-triplet transfer between the Chl and the carotenoids by TR-EPR (unpublished results). The interpretation of our data requires the knowledge of the magnetic properties of the triplet state of the Chl *d* pigment itself. Thus, the detection and characterization of Chl *d* triplet states in “natural” systems prompted us to study the optical/magnetic properties of the Chl *d* triplet states *in vitro*,

1
2 as a necessary step in order to be able to interpret the effect of the protein and the
3 interaction among pigments on the electronic properties of this pigment *in vivo*.
4

5
6 It is well known that aggregation effects in porphyrin related molecules depend on the
7 chromophore concentration and the characteristic of the solvents in which they are
8 dissolved. In this study we wanted to focus on the triplet state of monomeric Chl.
9
10 Therefore in order to avoid formation of dimers or even oligomers of the pigments, we
11 used very diluted samples (concentration below 10^{-5} M) throughout our investigations
12 both in the ZF-ODMR and the TR-EPR experiments. Actually the low temperature
13 fluorescence emission spectra indicate that Chl *a* and Chl *d* dimers or aggregates are not
14 formed in significant amount under our experimental conditions.
15
16

17
18 Me-THF is a highly polar solvent but a weak electron donor. In similar solvents, and at
19 low Chl concentrations, the Mg atom at the centre of porphyrin ring is expected to
20 assume a hexa-coordinated geometry. This is the least possible distorted conformation
21 of the macrocycle, the Mg atom lying substantially in the plane of the molecule. In
22 previous works both ZFS parameters and ESP of Chl *a* (and Chl *b*) have shown to be
23 dependent on the polarity of the solvent and on the penta/hexa ligation state of the
24 central magnesium. The general trend reported may be reassumed in the following: a
25 smaller D value and a reduced difference between the X, Y populating rates are
26 observed in non polar solvents [39]. The decrease of the absolute ZFS values observed
27 in hexa-coordinated Chls, in which two axial ligands donate to the central Mg atom,
28 compared to a penta-coordinated, single axial ligand, was interpreted as resulting from
29 an extension of the delocalization of the electronic spin distribution over the molecule
30 macrocycle [40]. In our experiments the TR-EPR and ZF-ODMR spectra of the Chl *a*
31 triplet state show the presence of only one triplet population. Comparison of the ZFS
32 parameters with literature data indicates that this species is likely a biligated Chl *a*
33 molecule: Chl *a*-(Me-THF)₂ [41,42]. The triplet spectra relative to Chl *d* are also
34
35
36
37
38
39
40
41
42
43
44
45
46
47
48
49
50
51
52
53
54
55
56
57
58
59
60

1
2 essentially due to a single triplet population and are also likely due to the biligated
3 species. As reported in table 1, the Chl *d* triplet state shows a 10% reduction of the
4 parameter D and a 10% increase of E, compared to the Chl *a* values. These changes are
5 probably due to the effect of replacing the divinyl group of Chl *a* with the formyl group
6 in ring A. In particular, the reduction of the absolute value of D can be satisfactorily
7 interpreted in terms of increased delocalization of the triplet state over the porphyrin
8 ring of Chl *d* compared to that of Chl *a*. The effect is opposite to the one produced by
9 the formyl group in ring B of Chl *b* in polar solvent with respect to Chl *a* [31]. The
10 relative populating probabilities of each of the three spin sublevels can be determined
11 by the initial ESP of the TR-EPR spectra. The population rates for the Chl *a* and *d*
12 triplet states in Me-THF, determined by our TR-EPR experiments, are reported in table
13 1. We found only minor differences between Chl *d* and Chl *a* populating rates, with a
14 small redistribution between the in plane components (X and Y). As in the case of Chl
15 *a*, also Chl *d* has the smallest component along Z, the out of plane component of the
16 dipolar tensor. Thus the active spin components lie in the porphyrin plane.

17
18 It has been suggested that the light modulation experiments may lead to incorrect
19 conclusions about the relative spin populations especially if the modulation frequency is
20 not high enough to reach the “fast limit” [29]. Therefore, TR-EPR gives more reliable
21 and accurate values for the initial population rates. We found however, for Chl *a*,
22 population rates very similar to those previously determined by CW-EPR using the
23 light-modulation technique, in the same solvent and at low concentrations [29].

24
25 The polarization pattern observed by steady-state FDMR for Chl *a* and *d* is slightly
26 different in the two cases, which may be indicative of a little difference in the decay
27 rates of the three triplet sublevels between the two species, in view of the fact that the
28 populating rates are quite similar, as demonstrated by TR-EPR. At 1.8 K, which is the
29 temperature of the FDMR experiments, the spin lattice relaxation becomes very slow
30
31
32
33
34
35
36
37
38
39
40
41
42
43
44
45
46
47
48
49
50
51
52
53
54
55
56
57
58
59
60

1
2 and the decay of the polarization depends only on the triplet sublevel decay rates. On
3
4 the other hand, in the TR-EPR experiments, which have been performed at 90 K, the
5
6 decay rates are not directly accessible due to the relatively fast spin-lattice relaxation
7
8 rate.
9

10 As already mentioned in the Results section, a second triplet population was detected by
11
12 FDMR in the Chl *d* samples even at very low concentrations, but only when the spectra
13
14 were recorded by monitoring the whole emission range, probably because this second
15
16 component is contributing mainly to the long tail of the fluorescence band. It is likely
17
18 that the minor triplet population is either the monoligated Chl *d* (Me-THF-Chl *d*) or a
19
20 dimeric form of Chl *d* (Chl *d*)₂. This last hypothesis is suggested by the selection at
21
22 higher fluorescence wavelengths of the component, however a shift toward higher
23
24 frequency as that observed would not be expected for dimers [41,42]. Similar effects
25
26 have been reported for Chl *b* in Me-THF [41,42]. We exclude the presence of impurities
27
28 such as pheophytin *d* or isochlorophyll *d*, which have been reported when the Chl *d*
29
30 pigment was dissolved in methanol, because the expected absorption peak at 660 nm in
31
32 the absorption spectrum [43] is missing (data not shown). The component was not
33
34 visible in the TR-EPR spectra, because this minor component is detectable only upon
35
36 optical selection using ODMR spectroscopy.
37
38
39

40 **5. Conclusions**

41
42 The change in the electronic structure, produced by the substitution of the divinyl group
43
44 by the formyl group in ring A in the Chl *d* pigment compared to Chl *a*, induces a large
45
46 red shift in the singlet absorption spectrum and only a minor difference in the triplet-
47
48 triplet absorption. The ZFS parameters and the ISC probabilities to the three spin
49
50 sublevels undergo a slight modification upon introduction of the formyl group.
51
52
53
54
55
56
57
58
59
60

1
2
3
4
5
6
7
8
9
10
11
12
13
14
15
16
17
18
19
20
21
22
23
24
25
26
27
28
29
30
31
32
33
34
35
36
37
38
39
40
41
42
43
44
45
46
47
48
49
50
51
52
53
54
55
56
57
58
59
60

In “normal” photosynthetic complexes Chls are typically penta-coordinated, with histidine acting as the principal axial donor. Hence, deviation of the ZFS parameter and the ESP pattern *in vivo*, compared to those determined here *in vitro* and assigned to biligated Chl *d* molecules, are expected. Obviously, further studies relating to the effect of solvent polarity and axial coordination are needed in order to fully understand the photo-physical properties of the triplet states of Chl *d*, both *in vitro* and *in vivo*. Nevertheless, based on our preliminary results, it can be argued that in a protein environment the behaviour of the Chl *d* triplet state will be very similar to that of Chl *a*. Therefore, the information acquired on the Chl *a* triplet state *in vivo* should be readily be transferred to Chl *d* binding complexes. Moreover, the formyl group of Chl *d* is in principle susceptible to H-bonding by specific protein residues (or appropriate organic solvents), providing an opportunity for nature to finely tune the electronic properties of the Chl *d* pigment population in order to attain both efficient energy transfer in the antenna and electron transfer in the reaction centres.

Acknowledgements

This work was supported by grants from the Italian Ministry for University and Research (MURST) under the project PRIN2005 and the U.K. Biotechnology and Biological Sciences Research Council (BBSRC, grant #B18658). S. S. would like to thank Y-K. Cheong (Queen Mary, University of London) for help in Chl *d* purification.

References

- [1] H. Miyashita, H. Ikemoto, N. Kurano, K. Adachi, M. Chihara and S. Miyachi, *Nature* **383**, 402 (1996).
- [2] Q. Hu, H. Miyashita, I. Iwasaki, N. Kurano, S. Miyachi, M. Iwaki and S. Itoh, *Proc. Natl. Acad. Sci. U. S. A.* **95**, 13319 (1998).
- [3] A. W. D. Larkum and M. Kuhl, *Trends in Plant Sci.* **10**, 355 (2005).
- [4] V. Sivakumar, R. L. Wang and G. Hastings, *Biophys. J.* **85**, 3162 (2003).
- [5] S. Santabarbara, G. Agostini, A. P. Casazza, C. D. Syme, P. Heathcote, F. Bohles, M. C. W. Evans, R. C. Jennings and D. Carbonera, *Biochim. Biophys. Acta-Bioenergetics* **1767**, 88 (2007).
- [6] T. Okubo, T. Noguchi, T. Tomo, H. Miyashita, T. Tsuchiya and M. Mimuro, *Plant and Cell Physiol.* **48**, S171 (2007).
- [7] E. Schlodder, M. Cetin, M. Eckert, H.J. Eckert, J. Barber and A. Telfer, *Biochim. Biophys. Acta* **1767**, 589 (2007).
- [8] A. S. Holt and H. V. Morley, *Can. J. Chem.* **37**, 507 (1959).
- [9] R. J. Ritchie, *Photosynth. Res.* **89**, 27 (2006).
- [10] J. C. Goedheer, in *The Chlorophylls.*; edited by L.P. Vernon, G.P. Seely, (Academic Press: New York, London, 1966).
- [11] J. Marquardt, E. Morschel, E. Rhiel and M. Westermann, *Arch. of Microbiol.* **174**, 181 (2000).
- [12] M. Kuhl, M. Chen, P. J. Ralph, U. Schreiber and A. W. D. Larkum, *Nature* **433**, 820 (2005).
- [13] S. Santabarbara, M. Chen, A.W.D. Larkum and M.C.W. Evans, *FEBS Lett.* **581**, 1567 (2007).
- [14] A. A. Krasnowsky, *Biophysics* **39**, 197 (1994).

- 1
2
3
4
5
6
7
8
9
10
11
12
13
14
15
16
17
18
19
20
21
22
23
24
25
26
27
28
29
30
31
32
33
34
35
36
37
38
39
40
41
42
43
44
45
46
47
48
49
50
51
52
53
54
55
56
57
58
59
60
- [15] H. Kramer and P. Mathis, *Biochim. Biophys. Acta* **593**, 319 (1980).
- [16] R. J. Cogdell, H. A. Frank, *Biochim. Biophys. Acta* **895**, 63 (1987).
- [17] E. Formaggio, G. Cinque and R. Bassi, *J. Mol. Biol.* **314**, 1157 (2001).
- [18] D. Siefermann-Harms and A. Angerhofer, *Photosynth. Res.* **55**, 83 (1998).
- [19] P. Mathis, W. L. Butler and K. Satoh, *Photochem. Photobiol.* **30**, 603 (1979).
- [20] D. Carbonera, G. Giacometti, G. Agostini, A. Angerhofer and V. Aust, *Chem. Phys. Lett.* **194**, 275 (1992).
- [21] E. J. G. Peterman, J. Dekker, R. Van Grondelle and H. Van Amerongen, *Biophys. J.* **69**, 2670 (1995).
- [22] D. Carbonera, G. Giacometti and G. Agostini, *Appl. Magn. Reson.* **3**, 361 (1992).
- [23] M.-L. Groot, E. J. G. Peterman, I. H. M. Van Stokkum, J. P. Dekker and R. Van Grondelle, *Biophys. J.* **68**, 281 (1995).
- [24] S. Santabarbara, E. Bordignon, R. C. Jennings and D. Carbonera, *Biochemistry* **41**, 8184 (2002).
- [25] R. Bearden and R. Malkin, *Biochim. Biophys. Acta* **283**, 456 (1972).
- [26] P. Setif, H. Bottin and P. Mathis, *Biochim. Biophys. Acta* **808**, 112 (1985).
- [27] W. A. Rutherford and J. E. Mullet, *Biochim. Biophys. Acta* **636**, 225 (1981).
- [28] F. J. E. Van Mieghem, W. Nitschke, P. Mathis and W. A. Rutherford, *Biochim. Biophys. Acta* **977**, 207 (1989).
- [29] M. C. Thurnauer, *Rev. Chem. Interm.* **3**, 197 (1979).
- [30] D. E. Budil and M. C. Thurnauer, *Biochim. Biophys. Acta* **1057**, 1 (1991).
- [31] R. H. Clarke, in *Triplet State ODMR Spectroscopy. Techniques and Applications to Biophysical Systems*; edited by R.H. Clarke, (Wiley-Interscience, New York, 1982).
- [32] A. Munznmaier, N. Rosch, S. Weber, C. Feller, E. Ohmes and G. Kothe, *J. Phys. Chem.* **96**, 10645 (1992).
- [33] A. J. Hoff, In *Advanced EPR*; edited by A.J. Hoff, (Elsevier, Amsterdam, 1989).

- 1
2 [34] D. Carbonera, G. Giacometti and G. Agostini, FEBS Lett. **343**, 200 (1994).
3
4 [35] S. Stoll and A. Schweiger, J. Magn. Reson. **178**, 42 (2006).
5
6 [36] R. P. Ilagan, T. W. Chapp, R. G. Hiller, F. P. Sharples, T. Polivka and H. A. Frank,
7
8 Photosynth. Res. **90**, 5 (2006).
9
10 [37] T. Polivka, R. G. Hiller and H. A. Frank, Arch. of Biochem. Biophys. **458**, 111
11
12 (2007).
13
14 [38] D. J. Miller, J. Catmull, R. Puskeiler, H. Tweedale, F. P. Sharples and R. G. Hiller,
15
16 Photosynth. Res. **86**, 229 (2005).
17
18 [39] I. Hiromitsu and L. Kevan, J. Phys. Chem. **92**, 2770 (1988).
19
20 [40] R. H. Clarke, S. Hotchandani, S. P. Jagannathan and R. M. Leblanc, Chem Phys
21
22 Lett. **89**, 37 (1982).
23
24 [41] W. Hagele, D. Schmid and H.C. Wolf, Z .Naturforsch. **33a**, 83 (1978).
25
26 [42] W. Hagele, D. Schmid and H. C. Wolf, Z .Naturforsch. **33a**, 94 (1978).
27
28 [43] W. M. Manning and H. H. Strain, J. Biol. Chem. **151**, 1 (1943).
29
30
31
32
33
34
35
36
37
38
39
40
41
42
43
44
45
46
47
48
49
50
51
52
53
54
55
56
57
58
59
60

1
2
3
4
5
6
7
8
9
10
11
12
13
14
15
16
17
18
19
20
21
22
23
24
25
26
27
28
29
30
31
32
33
34
35
36
37
38
39
40
41
42
43
44
45
46
47
48
49
50
51
52
53
54
55
56
57
58
59
60

**The Photoexcited Triplet State of Chlorophyll *d* in Methyl-
tetrahydrofuran studied by Optically Detected Magnetic Resonance
and Time-Resolved EPR**

Marilena Di Valentin^{a*}, Stefano Ceola^a, Giancarlo Agostini^b, Alison Telfer^d,
James Barber^d, Felix Böhles^c, Stefano Santabarbara^c, Donatella Carbonera^{a*}

^a*Dipartimento di Scienze Chimiche, Università di Padova, Via Marzolo 1,
35131, Padova, Italy*

^b*Consiglio Nazionale della Ricerca, Istituto di Chimica Biomolecolare,
Sezione di Padova, via Marzolo 1, 35131 Padova, Italy*

^c*School of Biological and Chemical Sciences, Queen Mary, University of
London, Mile End Road, E1 4NS, London, United Kingdom*

^d*Division of Molecular Biosciences, Imperial College London, Biochemistry
Building, South Kensington Campus, London SW7 2AZ, United Kingdom*

*to whom correspondence should be addressed:

e-mail: marilena.divalentin@unipd.it, donatella.carbonera@unipd.it

Abbreviations

Chl, chlorophyll; FDMR or ODMR, fluorescence or optically detected
magnetic resonance; PS, photosystem; TR-EPR, time resolved electron
paramagnetic resonance

Abstract

Chlorophyll *d* (Chl *d*) is the major pigment in the antenna proteins of both photosystems (PSI and II) of the oxyphotobacterium *Acaryochloris marina*. This fact suggests that photosynthesis based upon Chl *d* rather than Chl *a* may be an interesting alternative in oxygenic photosynthesis. While a great deal of spectroscopic information relative to Chl *a*, are available, both *in vivo* and *in vitro*, the literature on Chl *d* is scarce. In particular, the triplet state of Chl *d* has not been studied *in vitro* up to date. Although triplet states do not represent the main excitation path in the photosynthetic process they are involved in light stress events both in the antenna complexes and in the reaction centers and may also be used as endogenous paramagnetic probes of the molecular environment.

In this paper we make use of both time-resolved EPR and ODMR to characterize, for the first time, the Chl *d* triplet state in the polar solvent methyl-tetrahydrofuran. The comparison with the spectra of Chl *a* obtained under the same experimental conditions is also discussed.

Formatted

Formatted

Formatted

Formatted

Formatted

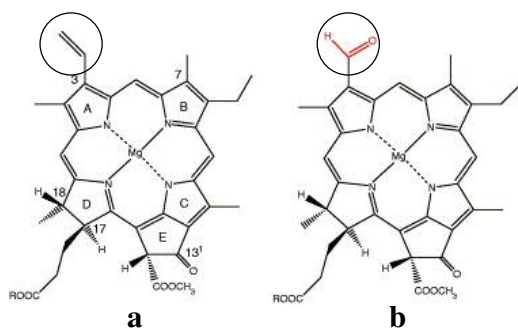
Formatted

1. Introduction

Chlorophyll (Chl *a*) is the dominant pigment in most oxygenic photosystems, acting both as a light harvesting pigment, in the inner and the peripheral antenna complexes, and as the primary electron donor in the reaction centres of Photosystem I (PSI) and Photosystem II (PSII). Chl *b* and *c* are found in the antenna complexes of higher plants and brown algae, respectively, but are not involved in photochemical pathways in the reaction centres. Hence, there has been a substantial consensus that Chl *a* is necessary to drive oxygenic photosynthesis. However, the ubiquitous role of Chl *a* has come under scrutiny when a the novel oxyphotobacterium *Acaryochloris marina* possessing Chl *d* in excess of 90% of the total chlorophyll was discovered [1]. Chl *d* in *A. marina* is not only the major pigment in the antenna proteins of both photosystems (PSI and II) [2] [3] but also acts as the primary donor in PSI, forming a special pair (either a Chl *d* dimer or a Chl *d*/Chl *d'* heterodimer) analogously to Chl *a* in PSI [2,4]. Despite the chemical difference in the primary donor in the PSI reaction centre of *A. marina* the kinetics of electron transfer and the chemical nature of secondary and successive electron transfer intermediates appear to be well conserved, compared to Chl *a* binding reaction centres of higher plants and cyanobacteria [5]. The role of Chl *d* in the reaction centre of *A. marina* is still a matter of debate. Evidence for Chl *d* acting as the primary donor has been recently reported by Okubo *et al.* [6]. On the other hand, Telfer and coworkers [7] suggested that it is Chl *a* which acts as the primary donor in PSII reaction centre of *A. marina*. However a role as an electron transfer intermediate for Chl *d* was not ruled out in this latter study. Hence, photosynthetic oxygen evolution based mainly upon Chl *d* rather than Chl *a* constitutes an interesting alternative in oxygenic photosynthesis.

1
2
3
4
5
6
7
8
9
10
11
12
13
14
15
16
17
18
19
20
21
22
23
24
25
26
27
28
29
30
31
32
33
34
35
36
37
38
39
40
41
42
43
44
45
46
47
48
49
50
51
52
53
54
55
56
57
58
59
60

In the Chl *d* molecule the divinyl group which is present in ring A of Chl *a* is replaced by a formyl group (Scheme 1). The proposed structure for Chl *d*, produced by oxidation as 2-desvinyl-2-formyl-chlorophyll-*a*, was provided in 1959 by Holt *et al.* [8]. Chl *d* differs markedly from all the other chlorophylls in having the Q_y absorption peak in the near infrared. The optical spectral properties of Chl *d* are, therefore, unique. The Q_y electronic transition of Chl *d* in acetone is characterized by an absorption peak at 691 [8-9], which is about 30 nm red-shifted compared to Chl *a* in the same organic solvent [10]. An even more pronounced red-shift of the absorption is observed *in vivo* where absorption transitions in the 708–720 nm range were observed [1]. Therefore, it has been hypothesised that the presence of Chl *d* as the principal pigment in *A. marina* is the result of adaptation to the peculiar environmental niche in which the organism resides, [2, 11], forming biofilms on the underside of didemnid ascidians [12]. This adaptation hypothesis is supported by the similarity of the electron transfer reactions in PSI of *A. marina* compared to those of Chl *a* binding organisms and the high homology of the all the reaction centre subunits [13]. In order to understand the role of the Chl *d* in energy transfer and electron transfer processes in the photosynthetic apparatus of *A.* it is necessary, in the first place, to acquire detailed information on the electronic and spectroscopic properties of Chl *d*.



1
2
3
4
5
6
7
8
9
Scheme 1. Molecular structure of (a) chlorophyll *a* and (b) chlorophyll *d*. The divinyl group in ring A of chlorophyll *a* is replaced by a formyl group in chlorophyll *d* (highlighted).

10
11
12
13
14
15
16
17
18
19
20
21
22
23
24
25
26
27
28
29
30
31
32
33
34
35
36
37
38
39
40
41
42
43
While singlet excited states of chlorophylls are directly involved in energy and electron transfer processes leading to energy conversion, excited triplet states do not take part in the main path of photosynthesis. Thus the Chl triplet, which in chlorophyll in organic solvent has a yield of around 60% (see [14] for a review), is of little direct importance in photosynthetic energy conversion. However, it plays a primary role during the light-induced stress, a phenomenon which goes under the name of photoinhibition. In the photosynthetic complexes, the triplet states of Chl are populated by two mechanisms; intersystem crossing (ISC) from the lowest singlet excited states, analogous to pigment in solution, and from charge recombination of the primary radical pair. The rate of ISC, in isolated pigment protein complexes, is significant and of the same order of magnitude as that for the other decay processes [15]. Although within chlorophyll protein complexes Chl triplet levels are normally efficiently quenched by carotenoids (e.g. [16-18]), Chl triplets populated by ISC have been detected in many PSII enriched particles [19] and components, including outer [20,21] and inner antenna [22,23] complexes. More recently Chl triplet states populated by ISC were also detected in substantially intact systems such as isolated thylakoid membranes from spinach [24] and *Chlamydomonas reinhardtii* [5].

44
45
46
47
48
49
50
51
52
53
54
55
56
57
58
59
60
In the reaction centres Chl triplet states can be populated by charge recombination of the separated primary radical pair couple [25-28]. Charge recombination reactions are enhanced by the pre-reduction of the terminal acceptors of the reaction centres. Under this condition the lifetime of the primary radical pair is lengthened by order of magnitudes (ns vs. ps timescale), increasing the probability of charge recombination,

1
2 and population of the triplet state [26-28]. Therefore Chl triplet states are molecular
3 probes of processes which occur under high excitation pressure, i.e. light stress
4 conditions. Since, triplet states are paramagnetic (total spin $S=1$) they are suited for
5 investigation by electron paramagnetic resonance (EPR) spectroscopic techniques.
6
7

8
9
10 Until now EPR investigations concerning the photo-excited triplet state of Chl *d* have
11 not been reported. On the other hand, the triplet states of Chl *a* and Chl *b*, both *in vivo*
12 and *in vitro*, have been the subject of extensive investigations either by optical or by
13 EPR spectroscopy. Many studies of the Chl triplet states have been performed with the
14 aim of understanding the environmental effect induced by solvent polarity and axial
15 ligand coordination to the central magnesium on the spectroscopic properties of the
16 molecules [29-31]. In most of the initial studies the steady-state EPR spectra of the Chl
17 triplet states were recorded by amplitude modulation of the light excitation beam and
18 phase-sensitive detection of the spin polarized spectrum, using a lock-in amplifier. More
19 recently the triplet state of Chl has been investigated by Time-resolved EPR (TR-EPR).
20 In TR-EPR experiments the resonant microwave field is directly monitored and the time
21 evolution of the spin-polarized spectrum after the laser pulse excitation is recorded [32].
22 TR-EPR allows the spin-polarization pattern (ESP) of a triplet state to be directly
23 determined, because it is conducted in the absence of external field modulation. The
24 ESP cannot be unambiguously determined by CW-EPR, due to the admixture of the
25 signals arising from spin-polarized (non-Boltzmann) and equilibrated (Boltzmann)
26 states.
27
28
29
30
31
32
33
34
35
36
37
38
39
40
41
42

43
44 The zero-field splitting (ZFS) tensor and ESP are the most important parameters of
45 triplet-state EPR. The ZFS parameters (D and E) reflect the intensity of the magnetic
46 dipolar interaction between the unpaired electrons. D is related to the mean distance
47 between spins while E is related to the symmetry of the electronic distribution in the
48 molecular plane. ESP depends on the selective ISC rates to the three spin sublevels.
49
50
51
52
53
54
55
56
57
58
59
60

1
2
3
4
5
6
7
8
9
10
11
12
13
14
15
16
17
18
19
20
21
22
23
24
25
26
27
28
29
30
31
32
33
34
35
36
37
38
39
40
41
42
43
44
45
46
47
48
49
50
51
52
53
54
55
56
57
58
59
60

Because the triplet sublevels are already not degenerate in the absence of an externally applied magnetic field due to the dipole-dipole magnetic interaction between the unpaired spins, Optically Detected Magnetic resonance in Zero-Field (ZF-ODMR) constitutes an alternative and complementary analytical tool to EPR for the study of photo-excited triplet states of chromophores. Thus, ZF-ODMR, has also been used extensively to characterize Chl triplet states both *in vitro* and in photosynthetic systems [31,33]. ZF-ODMR is a double resonance technique based on the simple principle that, when under continuous illumination a triplet steady state population is generated, the application of a resonant microwave field between a couple of spin sublevels of the triplet state generally induces a change of the steady state population of the triplet state itself, due to the anisotropy of the decay and population rates of the three spin sublevels. The change induced in the triplet population may be detected as a corresponding change in the emission and/or absorption of the system [31]. In the FDMR experiments the fluorescence is collected in the presence and in the absence of the swept microwave field and the difference is amplified. In the absorption detection mode (ADMR) the excitation beam is focused into the monochromator after passing through the sample and is finally collected by a photodiode. By fixing the microwave frequency at a resonant value while sweeping the detection wavelength, Triplet-minus-Singlet (T-S) spectra can be registered. The advantage of the technique is the high sensitivity due to the detection of optical photons and the possibility to correlate, by site selection, the ZFS parameters to the optical properties of the species carrying the triplet state. Because the anisotropy of electron spin-spin dipolar interaction does not contribute to the magnetic resonance linewidth in the absence of a magnetic field and the hyperfine interactions do not broaden the ODMR lines at the first order, the ZFS parameters can be determined with high precision. In fact the peaks at the resonant frequency are very narrow compared to EPR.

1
2
3
4
5
6
7
8
9
10
11
12
13
14
15
16
17
18
19
20
21
22
23
24
25
26
27
28
29
30
31
32
33
34
35
36
37
38
39
40
41
42
43
44
45
46
47
48
49
50
51
52
53
54
55
56
57
58
59
60

In this paper we make use of both TREPR and ODMR to characterize, for the first time, the Chl *d* triplet state in the polar solvent methyl-tetrahydrofuran (Me-THF). The comparison with the spectra of Chl *a* obtained under the same experimental conditions is also discussed.

We consider this an important starting point for the characterization and analysis of Chl *d* triplet states *in vivo*.

Formatted

2. Materials and Methods

Extraction and purification of Chl d from A. marina cells. *A. marina* was grown on K+ESM medium as previously described [7]. Cells were harvested in the logarithmic growth phase by centrifugation at 1 500 *g* for 10 minutes. Pigments were extracted by resuspending the cell pellet in methanol, with a volume equivalent to ten times the cells weight, for 20 minutes, at 4 C in the dark. The suspension was then centrifuged for 10 minutes at 12000 *g* in a refrigerated centrifuge. The procedure was repeated until the cell pellet was seemingly colourless. The green supernatants were pooled together and transferred in a separating flask. Pigments were separated by adding a volume equal to the initial methanol extract of diethyl ether. The solution was washed three times with equal volumes of water. The diethyl ether layer was dried in a rotary evaporator and the powder resuspended in a minimal amount of 45:45:10 Acetonitrile: Methanol: Water mixture. Chl *d* was purified by HPLC using an Agilent 1100 series HPLC integrated unit equipped with a on-line diode array detector. The pigment extract was loaded on a C18 reverse phase column (Spherisorb 5 μ m ODS2-C18 (Phase Separation Ltd, Deeside), dimension 250 x 4.1 mm) and the pigment were separated by running consecutive linear gradients. The first gradient starting mixture of 45:45:10 Acetonitrile: Methanol: Water, was run by decreasing the water content linearly, at a flow rate of 1ml min⁻¹, to 50:50 Acetonitrile: Methanol final mixture. The second gradient was run

1
2 increasing the Acetonitrile concentration to 80% at the same flow rate. The pigment
3 elution profile was monitored at 420nm, 500nm, 673 nm and 683nm simultaneously.

4
5
6 Chl *d* eluted with the second gradient after 23.5 minutes, and Chl *a* after 25.1 minutes.

7
8 The concentration and the purity of Chl *d* were checked by absorption spectroscopy
9 with a Lambda 35 Perkin Elmer spectrometer. Chl *a* was purchased from SIGMA; the
10 Chl was dried carefully before dissolving it in the Me-THF solvent to remove all
11 residual water. The solvent was distilled from sodium before usage.

12
13
14
15
16 *ODMR measurements.* The samples were diluted in Me-THF to a final Chl
17 concentration of 10^{-5} M sealed in a capillary tube after several pumping/freezing cycles
18 in order to remove the oxygen from the sample. Cooling of the samples was done
19 slowly down to cryogenic temperature in the cryostat. Fluorescence detected magnetic
20 resonance (FDMR) and absorption detected magnetic resonance (ADMR) experiments
21 were performed in the same, home built, apparatus, previously described in detail
22 [22,34]. The flexibility of the set up allows performance of both kinds of experiments
23 on the same sample by switching the detection mode. Amplitude modulation of the
24 applied microwave field, used to greatly increase the signal to noise ratio, was done by
25 means of a phase sensitive lock-in amplifier (EG&G 5220). In the FDMR experiments
26 the fluorescence, excited by a halogen lamp (250 W) focused into the sample and
27 filtered by a broadband 5 cm solution of CuSO_4 1M, was collected at 45 degree through
28 appropriate cut-on or band-pass filters (10 nm FWHM) by a photodiode before entering
29 the lock-in amplifier. Low temperature emission spectra were detected in the same
30 apparatus used for ODMR experiments, using the same excitation source, but
31 substituting the band-pass filters before the photodiode, coupled to a voltage-amplifier,
32 by a monochromator. In the ADMR setup the same excitation lamp was used but
33 without filters before the sample, except for 5 cm water and other heat filters. The beam
34 was focused into the monochromator after passing the sample and finally collected by a
35
36
37
38
39
40
41
42
43
44
45
46
47
48
49
50
51
52
53
54
55
56
57
58
59
60

1
2 photodiode. The temperature was 1.8 K for most of the experiments. At such a
3
4 temperature spin-lattice relaxation is inhibited and the ODMR signal is maximum.
5

6
7 *TR-EPR measurements.* TR-EPR spectra were obtained in quadrature detection mode
8
9 with DC-AFC coupling using pulsed light excitation. The X-band EPR spectrometer
10
11 (Bruker Elexsys E580) was equipped with a EN4118X-MD4 X-band dielectric module
12
13 working at 9.7 GHz and a nitrogen flow system. The EPR experiments were performed
14
15 at 90 K. . The microwave power used for the TR-EPR experiments was about 2mW at
16
17 the cavity. Laser excitation at 532nm (10 mJ per pulse and repetition rate of 10 Hz) was
18
19 provided by the second harmonic of a Nd:YAG laser (Quantel Brilliant).
20

21
22 The time resolution of the TR-EPR spectrometer was 100 ns. No field modulation or
23
24 phase-sensitive detection was used. The EPR signals were taken from the quadrature
25
26 detection arm of the Super XFT bridge and sampled with the SpecJet, triggered by the
27
28 Q-switch. Transients were accumulated under off-resonance field conditions and
29
30 subtracted from those on resonance in order to eliminate the laser background signal.

Formatted

31
32 Simulations of the spin polarised triplet spectra were performed using a program written
33
34 in Matlab® with the aid of the Easyspin routine (ver. 2.6.0) [35].The program is based
35
36 on the full diagonalization of the spin Hamiltonian, taking into account the Zeeman and
37
38 magnetic dipole-dipole interactions, assuming a powder distribution of molecular
39
40 orientations with respect to the magnet field direction.
41

42 43 44 **3. Results**

45
46 The fluorescence emission spectra of Chl *d* and Chl *a* dissolved in Me-THF, detected at
47
48 1.8 K, are presented in figure 1. The fluorescence emission spectra of Chl *a* peaks at
49
50 673 nm and shows an intense low-energy vibrational band at 727 nm. The main
51
52 fluorescence emission band and the low-energy vibrational transition are red-shifted to
53
54
55
56
57
58
59
60

698 nm and 760 nm respectively, in the fluorescence emission spectrum of Chl *d*. The red shift of the Chl *d* fluorescence emission compared to that of Chl *a* is in agreement with previous observations of the emission spectra of these pigments recorded at 10 K in reconstituted complex of PCP [36]. It is also in agreement with the absorption spectrum of the pigments at 10 K in Me-THF which shows the main electronic transition at 670 nm for Chl *a* and at 697 nm for Chl *d* [36].

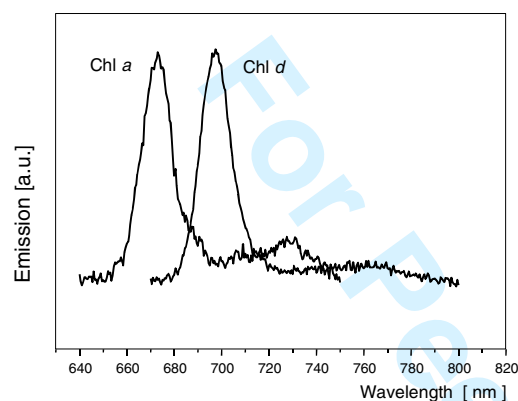


Figure 1. Normalized fluorescence emission spectra of Chl *a* and Chl *d* in Me-THF at 1.8 K. Broad band excitation (400-600 nm), resolution 1 nm.

The FDMR spectra taken at the maximum of the fluorescence are shown in figure 2. Only two of the three possible transitions were detected. They correspond to the $|D|-|E|$ and $|D|+|E|$ transitions. The $2|E|$ transition was too weak to be detected, as usually reported for Chl *a* and *b* triplet states. The $|D|-|E|$ transition of Chl *a* in Me-THF has a maximum at 740 MHz, while the $|D|+|E|$ transition shows a peak at 992 MHz. Instead, the $|D|-|E|$ transition of Chl *d* has a peak at 616 MHz, downshifted by 124 MHz compared to Chl *a*. As the linewidth (FWHM) of the $|D|-|E|$ resonance lines of Chl *a* and Chl *d* are 37.5 MHz and 40 MHz respectively, the two transitions do not overlap, and would be distinguishable in a Chl *a*/Chl *d* mixture, as it occurs *in vivo*. The $|D|+|E|$ transition of Chl *d* is observed at 906 MHz, and it is less separated from that of Chl *a*.

The corresponding ZFS parameters for both species are reported in table 1. The order of relative intensity of the transitions is the same for the two pigments, that is $|D|-|E| > |D|+|E| >> 2|E|$, although the difference among them is more pronounced for the Chl *d* triplet state.

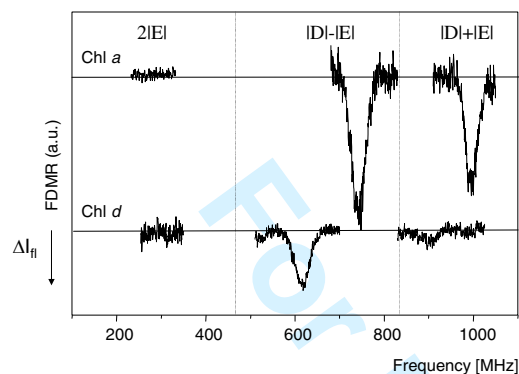


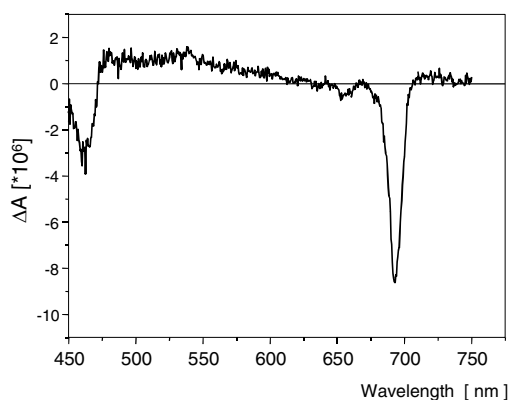
Figure 2. FDMR spectra of Chl *a* and Chl *d* in Me-THF at 1.8 K collected through a 10 nm band pass filter at emission wavelength near the maximum of the emission spectral forms shown in Figure 1: 670 nm for Chl *a* and 700 nm for Chl *d*. Spectral regions corresponding to $2|E|$, $|D|-|E|$, $|D|+|E|$ transitions are indicated. Microwave frequency modulation: 33 Hz; Microwave power, 0.6 mW. Number of scans: 30. The traces have been vertically shifted for an easier comparison.

ODMR					
	$ D - E $ (MHz)	$ D + E $ (MHz)	FWHM (MHz)	$ D $ (cm^{-1})	$ E $ (cm^{-1})
Chl <i>a</i>	740.0 ± 0.5	992.0 ± 0.5	40.0 ± 0.5	0.0289	0.0042
Chl <i>d</i>	616.0 ± 0.5	906.0 ± 0.5	40.5 ± 0.5	0.0254	0.0048
EPR					
	A_x	A_y	A_z	$ D $ (cm^{-1})	$ E $ (cm^{-1})
Chl <i>a</i>	0.33	0.56	0.11	0.0289	0.0042
Chl <i>d</i>	0.34	0.50	0.16	0.0259	0.0050

Table 1. ODMR: values of experimental resonant frequencies and of the calculated ZFS parameters (errors $\pm 0.0001 \text{ cm}^{-1}$).

TR-EPR: Relative population probabilities (A_x , A_y , A_z) and ZFS parameters (errors $\pm 0.0002 \text{ cm}^{-1}$) determined from spectral simulations.

By setting the resonance frequency at 616 MHz, the maximum value of the $|D| - |E|$ transition, the microwave-induced T-S spectrum of Chl *d* was recorded (see figure 3). The main absorption bleaching is centred at 693 nm and corresponds to the Q_y transition in the singlet manifold, while a bleaching in the Soret region is seen below 470 nm (close to the wavelength limit of the monochromator). The positive triplet-triplet absorption is a broad band covering the range between 450 and 700 nm. The general features of the T-S spectrum are very similar to those reported for Chl *a* in monomeric form [33], indicating that the main electronic structure of the Chl *d* triplet manifold is conserved with respect to Chl *a*. The absence of a positive contribution to the T-S spectrum in the region of the Q_y absorption is an indication that the species associated to the magnetic transition is not a Chl *d* dimer.



1
2
3
4
5
6
7
8
9
10
11
12
13
14
15
16
17
18
19
20
21
22
23
24
25
26
27
28
29
30
31
32
33
34
35
36
37
38
39
40
41
42
43
44
45
46
47
48
49
50
51
52
53
54
55
56
57
58
59
60

Figure 3. T-S spectrum of Chl *d* in Me-THF at 1.8 K detected at 616 MHz, the maximum of the $|D|-|E|$ transition detected by FDMR. Mod. freq. 323 Hz, Mw power 1W.

The ADMR spectrum obtained by selecting a detection wavelength at 693 nm, (the maximum bleach in the T-S spectrum) is presented in figure 4. It shows the same microwave transitions detected by FDMR, with the same relative intensity, confirming that the same triplet population is observed either by absorption or fluorescence emission.

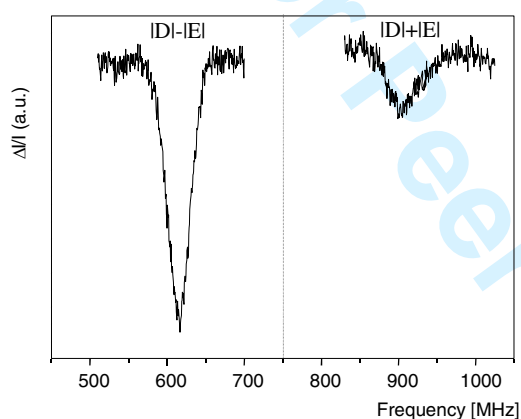


Figure 4. ADMR spectrum of Chl *d* in Me-THF at 1.8 K, recorded at 692.5 nm. Mod. freq. 33 Hz, Mw power 1W. Only the $|D|-|E|$, $|D|+|E|$ transitions are shown.

When performing FDMR on the Chl *d* triplet state by collecting the whole emission band (using a 650 nm cut-on filter) an additional peak at about 940 MHz, with opposite sign compared to that detected by the band pass filter at 700 nm, shows up (see figure 5). A corresponding $|D|-|E|$ transition is however not easily discerned in the spectrum. This additional transition may be due to the presence of a second minor population of triplet state. Unfortunately we were unable to measure either a specific emission

wavelength or an associated T-S spectrum of this second component because of the weakness of the corresponding signal.

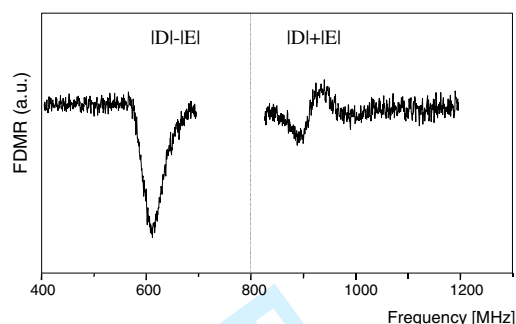


Figure 5. FDMR spectra of Chl *d* in Me-THF at 1.8 K, collected through a 630 nm cut-off filter. Spectral regions corresponding to $|D|-|E|$ and $|D|+|E|$ transitions are indicated. Microwave frequency modulation: 33 Hz; Microwave power, 0.6 mW. Number of scans: 25.

The laser-flash induced TR-EPR spectrum of Chl *d* in Me-THF at 90 K is shown in figure 6. The spectrum, recorded at 100ns after the laser flash, with an integration window of 60 ns, can be considered the initial spectrum, from the point of view of the ESP, because decay rate of the EPR transient signals is in microsecond range at low microwave power (data not shown). The polarization pattern of this initial powder spectrum is *eaeeae*. The ZFS parameters $|D|$ and $|E|$, obtained from spectral simulation, are in good agreement with the values derived from the ODMR experiments for the main triplet population. A comparison with the spectrum of Chl *a*, obtained in the same experimental conditions, is also shown in the same figure. The population probabilities at the three canonical field positions (X,Y,Z) and the ZFS parameters, obtained from the spectral simulations of the initial triplet spectra (shown in figure 6), are reported in table 1 for both molecules.

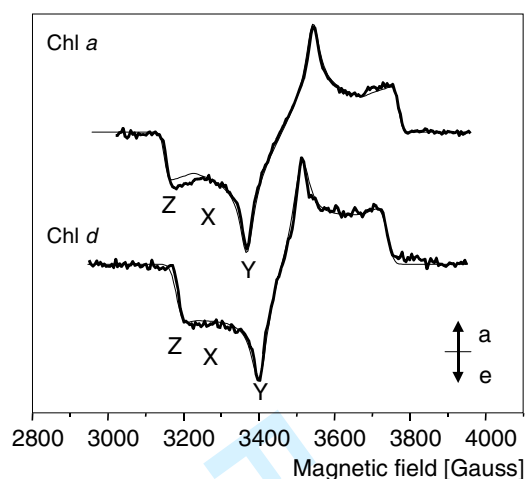


Figure 6. X-band triplet TREPR spectra of Chl *a* (top) and Chl *d* (bottom) in Me-THF at 100 ns after the laser pulse (thick line) and the corresponding spectral simulations (thin line). The simulation parameters are reported in table 1. *a* = absorption, *e* = emission.

4. Discussion

As already stated in the Introduction, the discovery of the photosynthetic oxygenic organism *Acaryochloris marina*, containing Chl *d* rather than Chl *a* as its major pigment, has challenged the view that Chl *a* is necessary in order to perform oxygen evolution. Moreover, very recently the PCP antenna complex from the red alga *Dinoflagellate*, which contains two Chl *a* molecules surrounded by 8 peridinin, has been reconstituted *in vitro* with Chl *d*, to study the effect of the porphyrin electronic structure on the efficiency of the energy transfer [36-38]. We have studied this reconstituted complex in terms of triplet-triplet transfer between the Chl and the carotenoids by TR-EPR (unpublished results). The interpretation of our data requires the knowledge of the magnetic properties of the triplet state of the Chl *d* pigment itself. Thus, the detection and characterization of Chl *d* triplet states in “natural” systems prompted us to study the optical/magnetic properties of the Chl *d* triplet states *in vitro*,

1
2
3
4
5
6
7
8
9
10
11
12
13
14
15
16
17
18
19
20
21
22
23
24
25
26
27
28
29
30
31
32
33
34
35
36
37
38
39
40
41
42
43
44
45
46
47
48
49
50
51
52
53
54
55
56
57
58
59
60

as a necessary step in order to be able to interpret the effect of the protein and the interaction among pigments on the electronic properties of this pigment *in vivo*.

It is well known that aggregation effects in porphyrin related molecules depend on the chromophore concentration and the characteristic of the solvents in which they are dissolved. In this study we wanted to focus on the triplet state of monomeric Chl. Therefore in order to avoid formation of dimers or even oligomers of the pigments, we used very diluted samples (concentration below 10^{-5} M) throughout our investigations both in the ZF-ODMR and the TR-EPR experiments. Actually the low temperature fluorescence emission spectra indicate that Chl *a* and Chl *d* dimers or aggregates are not formed in significant amount under our experimental conditions.

Me-THF is a highly polar solvent but a weak electron donor. In similar solvents, and at low Chl concentrations, the Mg atom at the centre of porphyrin ring is expected to assume a hexa-coordinated geometry. This is the least possible distorted conformation of the macrocycle, the Mg atom lying substantially in the plane of the molecule. In previous works both ZFS parameters and ESP of Chl *a* (and Chl *b*) have shown to be dependent on the polarity of the solvent and on the penta/hexa ligation state of the central magnesium. The general trend reported may be reassumed in the following: a smaller D value and a reduced difference between the X, Y populating rates are observed in non polar solvents [39]. The decrease of the absolute ZFS values observed in hexa-coordinated Chls, in which two axial ligands donate to the central Mg atom, compared to a penta-coordinated, single axial ligand, was interpreted as resulting from an extension of the delocalization of the electronic spin distribution over the molecule macrocycle [40]. In our experiments the TR-EPR and ZF-ODMR spectra of the Chl *a* triplet state show the presence of only one triplet population. Comparison of the ZFS parameters with literature data indicates that this species is likely a biligated Chl *a* molecule: Chl *a*-(Me-THF)₂ [41,42]. The triplet spectra relative to Chl *d* are also

1
2 essentially due to a single triplet population and are also likely due to the biligated
3 species. As reported in table 1, the Chl *d* triplet state shows a 10% reduction of the
4 parameter D and a 10% increase of E, compared to the Chl *a* values. These changes are
5 probably due to the effect of replacing the divinyl group of Chl *a* with the formyl group
6 in ring A. In particular, the reduction of the absolute value of D can be satisfactorily
7 interpreted in terms of increased delocalization of the triplet state over the porphyrin
8 ring of Chl *d* compared to that of Chl *a*. The effect is opposite to the one produced by
9 the formyl group in ring B of Chl *b* in polar solvent with respect to Chl *a* [31]. The
10 relative populating probabilities of each of the three spin sublevels can be determined
11 by the initial ESP of the TR-EPR spectra. The population rates for the Chl *a* and *d*
12 triplet states in Me-THF, determined by our TR-EPR experiments, are reported in table
13 1. We found only minor differences between Chl *d* and Chl *a* populating rates, with a
14 small redistribution between the in plane components (X and Y). As in the case of Chl
15 *a*, also Chl *d* has the smallest component along Z, the out of plane component of the
16 dipolar tensor. Thus the active spin components lie in the porphyrin plane.

17
18 It has been suggested that the light modulation experiments may lead to incorrect
19 conclusions about the relative spin populations especially if the modulation frequency is
20 not high enough to reach the “fast limit” [29]. Therefore, TR-EPR gives more reliable
21 and accurate values for the initial population rates. We found however, for Chl *a*,
22 population rates very similar to those previously determined by CW-EPR using the
23 light-modulation technique, in the same solvent and at low concentrations [29].

24
25 The polarization pattern observed by steady-state FDMR for Chl *a* and *d* is slightly
26 different in the two cases, which may be indicative of a little difference in the decay
27 rates of the three triplet sublevels between the two species, in view of the fact that the
28 populating rates are quite similar, as demonstrated by TR-EPR. At 1.8 K, which is the
29 temperature of the FDMR experiments, the spin lattice relaxation becomes very slow
30
31
32
33
34
35
36
37
38
39
40
41
42
43
44
45
46
47
48
49
50
51
52
53
54
55
56
57
58
59
60

1
2 and the decay of the polarization depends only on the triplet sublevel decay rates. On
3
4 the other hand, in the TR-EPR experiments, which have been performed at 90 K, the
5
6 decay rates are not directly accessible due to the relatively fast spin-lattice relaxation
7
8 rate.
9

10 As already mentioned in the Results section, a second triplet population was detected by
11
12 FDMR in the Chl *d* samples even at very low concentrations, but only when the spectra
13
14 were recorded by monitoring the whole emission range, probably because this second
15
16 component is contributing mainly to the long tail of the fluorescence band. It is likely
17
18 that the minor triplet population is either the monoligated Chl *d* (Me-THF-Chl *d*) or a
19
20 dimeric form of Chl *d* (Chl *d*)₂. This last hypothesis is suggested by the selection at
21
22 higher fluorescence wavelengths of the component, however a shift toward higher
23
24 frequency as that observed would not be expected for dimers [41,42]. Similar effects
25
26 have been reported for Chl *b* in Me-THF [41,42]. We exclude the presence of impurities
27
28 such as pheophytin *d* or isochlorophyll *d*, which have been reported when the Chl *d*
29
30 pigment was dissolved in methanol, because the expected absorption peak at 660 nm in
31
32 the absorption spectrum [43] is missing (data not shown). The component was not
33
34 visible in the TR-EPR spectra, because this minor component is detectable only upon
35
36 optical selection using ODMR spectroscopy.
37
38
39

40 **5. Conclusions**

41
42 The change in the electronic structure, produced by the substitution of the divinyl group
43
44 by the formyl group in ring A in the Chl *d* pigment compared to Chl *a*, induces a large
45
46 red shift in the singlet absorption spectrum and only a minor difference in the triplet-
47
48 triplet absorption. The ZFS parameters and the ISC probabilities to the three spin
49
50 sublevels undergo a slight modification upon introduction of the formyl group.
51
52
53
54
55
56
57
58
59
60

1
2
3
4
5
6
7
8
9
10
11
12
13
14
15
16
17
18
19
20
21
22
23
24
25
26
27
28
29
30
31
32
33
34
35
36
37
38
39
40
41
42
43
44
45
46
47
48
49
50
51
52
53
54
55
56
57
58
59
60

In “normal” photosynthetic complexes Chls are typically penta-coordinated, with histidine acting as the principal axial donor. Hence, deviation of the ZFS parameter and the ESP pattern *in vivo*, compared to those determined here *in vitro* and assigned to biligated Chl *d* molecules, are expected. Obviously, further studies relating to the effect of solvent polarity and axial coordination are needed in order to fully understand the photo-physical properties of the triplet states of Chl *d*, both *in vitro* and *in vivo*. Nevertheless, based on our preliminary results, it can be argued that in a protein environment the behaviour of the Chl *d* triplet state will be very similar to that of Chl *a*. Therefore, the information acquired on the Chl *a* triplet state *in vivo* should be readily be transferred to Chl *d* binding complexes. Moreover, the formyl group of Chl *d* is in principle susceptible to H-bonding by specific protein residues (or appropriate organic solvents), providing an opportunity for nature to finely tune the electronic properties of the Chl *d* pigment population in order to attain both efficient energy transfer in the antenna and electron transfer in the reaction centres.

Acknowledgements

This work was supported by grants from the Italian Ministry for University and Research (MURST) under the project PRIN2005 and the U.K. Biotechnology and Biological Sciences Research Council (BBSRC, grant #B18658). S. S. would like to thank Y-K. Cheong (Queen Mary, University of London) for help in Chl *d* purification.

References

- [1] H. Miyashita, H. Ikemoto, N. Kurano, K. Adachi, M. Chihara and S. Miyachi, *Nature* **383**, 402 (1996).
- [2] Q. Hu, H. Miyashita, I. Iwasaki, N. Kurano, S. Miyachi, M. Iwaki and S. Itoh, *Proc. Natl. Acad. Sci. U. S. A.* **95**, 13319 (1998).
- [3] A. W. D. Larkum and M. Kuhl, *Trends in Plant Sci.* **10**, 355 (2005).
- [4] V. Sivakumar, R. L. Wang and G. Hastings, *Biophys. J.* **85**, 3162 (2003).
- [5] S. Santabarbara, G. Agostini, A. P. Casazza, C. D. Syme, P. Heathcote, F. Bohles, M. C. W. Evans, R. C. Jennings and D. Carbonera, *Biochim. Biophys. Acta-Bioenergetics* **1767**, 88 (2007).
- [6] T. Okubo, T. Noguchi, T. Tomo, H. Miyashita, T. Tsuchiya and M. Mimuro, *Plant and Cell Physiol.* **48**, S171 (2007).
- [7] E. Schlodder, M. Cetin, M. Eckert, H.J. Eckert, J. Barber and A. Telfer, *Biochim. Biophys. Acta* **1767**, 589 (2007).
- [8] A. S. Holt and H. V. Morley, *Can. J. Chem.* **37**, 507 (1959).
- [9] R. J. Ritchie, *Photosynth. Res.* **89**, 27 (2006).
- [10] J. C. Goedheer, in *The Chlorophylls.*; edited by L.P. Vernon, G.P. Seely, (Academic Press: New York, London, 1966).
- [11] J. Marquardt, E. Morschel, E. Rhiel and M. Westermann, *Arch. of Microbiol.* **174**, 181 (2000).
- [12] M. Kuhl, M. Chen, P. J. Ralph, U. Schreiber and A. W. D. Larkum, *Nature* **433**, 820 (2005).
- [13] S. Santabarbara, M. Chen, A.W.D. Larkum and M.C.W. Evans, *FEBS Lett.* **581**, 1567 (2007).
- [14] A. A. Krasnowsky, *Biophysics* **39**, 197 (1994).

- 1
2 [15] H. Kramer and P. Mathis, *Biochim. Biophys. Acta* **593**, 319 (1980).
3
4 [16] R. J. Cogdell, H. A. Frank, *Biochim. Biophys. Acta* **895**, 63 (1987).
5
6 [17] E. Formaggio, G. Cinque and R. Bassi, *J. Mol. Biol.* **314**, 1157 (2001).
7
8 [18] D. Siefermann-Harms and A. Angerhofer, *Photosynth. Res.* **55**, 83 (1998).
9
10 [19] P. Mathis, W. L. Butler and K. Satoh, *Photochem. Photobiol.* **30**, 603 (1979).
11
12 [20] D. Carbonera, G. Giacometti, G. Agostini, A. Angerhofer and V. Aust, *Chem.*
13
14 *Phys. Lett.* **194**, 275 (1992).
15
16 [21] E. J. G. Peterman, J. Dekker, R. Van Grondelle and H. Van Amerongen, *Biophys.*
17
18 *J.* **69**, 2670 (1995).
19
20 [22] D. Carbonera, G. Giacometti and G. Agostini, *Appl. Magn. Reson.* **3**, 361 (1992).
21
22 [23] M.-L. Groot, E. J. G. Peterman, I. H. M. Van Stokkum, J. P. Dekker and R. Van
23
24 Grondelle, *Biophys. J.* **68**, 281 (1995).
25
26 [24] S. Santabarbara, E. Bordignon, R. C. Jennings and D. Carbonera, *Biochemistry* **41**,
27
28 8184 (2002).
29
30 [25] R. Bearden and R. Malkin, *Biochim. Biophys. Acta* **283**, 456 (1972).
31
32 [26] P. Setif, H. Bottin and P. Mathis, *Biochim. Biophys. Acta* **808**, 112 (1985).
33
34 [27] W. A. Rutherford and J. E. Mullet, *Biochim. Biophys. Acta* **636**, 225 (1981).
35
36 [28] F. J. E. Van Mieghem, W. Nitschke, P. Mathis and W. A. Rutherford, *Biochim.*
37
38 *Biophys. Acta* **977**, 207 (1989).
39
40 [29] M. C. Thurnauer, *Rev. Chem. Interm.* **3**, 197 (1979).
41
42 [30] D. E. Budil and M. C. Thurnauer, *Biochim. Biophys. Acta* **1057**, 1 (1991).
43
44 [31] R. H. Clarke, in *Triplet State ODMR Spectroscopy. Techniques and Applications to*
45
46 *Biophysical Systems*; edited by R.H. Clarke, (Wiley-Interscience, New York:, 1982).
47
48 [32] A. Munznmaier, N. Rosch, S. Weber, C. Feller, E. Ohmes and G. Kothe, *J. Phys.*
49
50 *Chem.* **96**, 10645 (1992).
51
52 [33] A. J. Hoff, In *Advanced EPR*; edited by A.J. Hoff, (Elsevier, Amsterdam, 1989).
53
54
55
56
57
58
59
60

- 1
2
3 [34] D. Carbonera, G. Giacometti and G. Agostini, FEBS Lett. **343**, 200 (1994).
4
5 [35] S. Stoll and A. Schweiger, J. Magn. Reson. **178**, 42 (2006).
6
7 [36] R. P. Ilagan, T. W. Chapp, R. G. Hiller, F. P. Sharples, T. Polivka and H. A. Frank,
8
9 Photosynth. Res. **90**, 5 (2006).
10
11 [37] T. Polivka, R. G. Hiller and H. A. Frank, Arch. of Biochem. Biophys. **458**, 111
12
13 (2007).
14
15 [38] D. J. Miller, J. Catmull, R. Puskeiler, H. Tweedale, F. P. Sharples and R. G. Hiller,
16
17 Photosynth. Res. **86**, 229 (2005).
18
19 [39] I. Hiromitsu and L. Kevan, J. Phys. Chem. **92**, 2770 (1988).
20
21 [40] R. H. Clarke, S. Hotchandani, S. P. Jagannathan and R. M. Leblanc, Chem Phys
22
23 Lett. **89**, 37 (1982).
24
25 [41] W. Hagele, D. Schmid and H.C. Wolf, Z .Naturforsch. **33a**, 83 (1978).
26
27 [42] W. Hagele, D. Schmid and H. C. Wolf, Z .Naturforsch. **33a**, 94 (1978).
28
29 [43] W. M. Manning and H. H. Strain, J. Biol. Chem. **151**, 1 (1943).
30
31
32
33
34
35
36
37
38
39
40
41
42
43
44
45
46
47
48
49
50
51
52
53
54
55
56
57
58
59
60